INVESTIGATIONS OF THE CONDUCTOR-SEMICONDUCTOR INTERFACE

Thesis by

Robert A. Scranton

In Partial Fulfillment of the Requirements

for the Degree of

Doctor of Philosophy

California Institute of Technology

Pasadena, California

1978

(Submitted October 19, 1977)

To my father

ACKNOWLEDGMENTS

I am deeply indebted to J. O. McCaldin for his interest, guidance and encouragement during my graduate studies. I appreciate the assistance of T. C. McGill, especially for the discussions on solid state physics. C. A. Mead generously shared his knowledge of experimental technique and his laboratory. J. S. Best helped in numerous ways. The greatest pleasure of my years at CalTech was working with these four men, who provided the bulk of my graduate education.

Special thanks are due J. B. Mooney for his assistance in $(SN)_x$ synthesis and deposition.

F. B. Humphrey, C. A. Mead, A. Yariv, F. A. Kroger, D. E. Hill, S. Nagata, and W. P. Allred supplied some of the crystals used in this work. The Jet Propulsion Laboratory (NASA) permitted use of their facilities. I thank the Corning Glass Foundation for a fellowship, and Ford-Exxon, the Office of Naval Research, the Army Research Office, and CalTech for funding.

ABSTRACT

I. Schottky barriers produced by polymeric sulfur nitride, $(SN)_x$, on nine common III-V and II-VI compound semiconductors are compared to barriers formed by Au. The conductor $(SN)_x$ produces significantly higher barriers to n-type semiconductors and lower barriers to p-type semiconductors than Au, the most electronegative elemental metal. The barrier height improvement, defined as $\phi_{(SN)_x} - \phi_{(Au)}$, is smaller on covalent semiconductors than on ionic semiconductors; $(SN)_x$ barriers follow the ionic-covalent transition. Details of $(SN)_x$ film deposition, samples preparation, and barrier height measurements are described.

II. The rate of dissolution of amorphous Si into solid Al is measured. The rate of movement of the amorphous Si/Al interface is found to be much faster than predicted by a simple model of the transport of Si through Al. This result is related to defects in the growth of epitaxial Si using the solid phase epitaxy process.

Parts of this thesis have been published or presented under the following titles.

Highly Electronegative Metallic Contacts to Semiconductors Using Polymeric Sulfur Nitride by R. A. Scranton, J. B. Mooney, J. O. McCaldin, T. C. McGill and C. A. Mead, Appl. Phys. Lett. 29, 47 (1976)

Highly Electronegative Contacts to Compound Semiconductors by R. A. Scranton, J. S. Best, and J. O. McCaldin, J. Vac, Sci. Technol. 14, 930 (1977)

The Schottky Barriers Produced by Polymeric Sulfur Nitride on Compound Semiconductors by R. A. Scranton, J. Appl. Phys. 48, 3838 (1977)

Highly Electronegative Contacts to Compound Semiconductors (invited talk), presented by R. A. Scranton at the 4th Annual Conference on the Physics of Compound Semiconductor Interfaces, Princeton, New Jersey Feb. 8, 1977

TABLE OF CONTENTS

I. The Schottky Barriers Formed by Polymeric Sulfur Nitride on Compound Semiconductors.

A. Introduction

At an intimate conductor-semiconductor interface, i.e., a Schottky barrier, there exists a reproduceable energy relationship between the Fermi level of the conductor and the valence band maximum and conduction band minimum of the semiconductor. The electrical behavior of such an interface is often characterized by a single parameter, the barrier height,[1] ϕ.

Conductor-semiconductor interfaces are an essential part of many semiconductor devices.[2] Large barriers, with resultant high electric fields, are useful for charge separation and for the control of the flow of charge carriers. Small barriers are useful for ohmic contacts. Schottky barriers are potentially useful for semiconducting materials in which the standard method for producing ohmics and controlling charge flow, namely, the introduction of controlled concentrations of ionized impurity atoms, is difficult.

The relation between the barrier height and the energy bands at the interface can be visualized by means of a band diagram (see fig. 1). The barrier for holes, ϕ_p, is the potential difference between the semiconductor valence band maximum at the interface and the conductor Fermi level as depicted in Fig. 1b. It is independent of semi-

Figure 1. At intimate conductor-semiconductor contacts (a), the positions of the conduction band minimum, C. B., conductor Fermi level, E_F, and valence band maximum, V. B., are independent of semiconductor doping. Thus ϕ_P, the barrier on p-type semiconductor (b), plus ϕ_N, the barrier on n-type semiconductors (c), sum to E_G, the band gap energy.

(a)

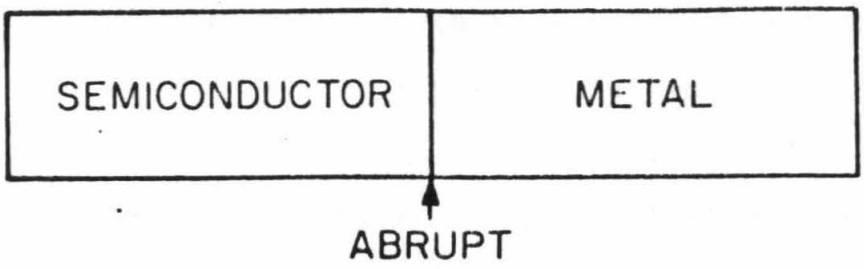

(b)

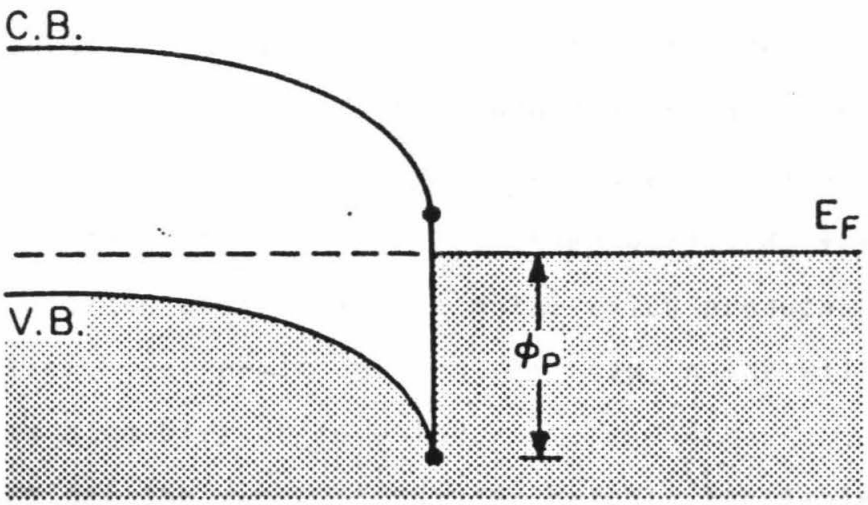

(c)

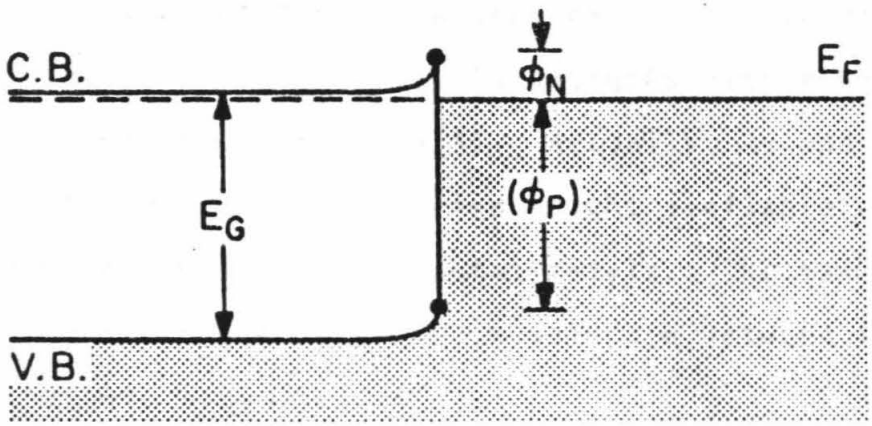

(d) $\phi_N + \phi_P = E_G$

conductor doping as can be seen by supposing that the Fermi level in the bulk of the semiconductor is brought closer to the conduction band, as in Fig. 1c. The barrier height for electrons, ϕ_n, is the potential difference between the conduction band minimum at the interface and the conductor Fermi level. Note that as the doping changes, the positions of the conduction band minimum, the conductor Fermi level, and valence band maximum at the interface do not change. In other words, $\phi_n + \phi_p = E_G$, where E_G is the energy gap. A metal which produces a very low barrier, i.e. ohmic contact, to, say, n-InP will produce a high barrier to p-InP.

Consider the range of barrier heights available with elemental metals. Figure 2 compares the Al/n-ZnS barrier with the Au/n-ZnS barrier. Au produces higher barriers to n-ZnS than Al. In general, Au produces higher barriers to n-type semiconductors than Al. Actually, Au and Al represent the extremes of barrier height available using the common, non-reactive elemental metals. The barrier heights for other commonly used metals lie between the barrier heights for Au and Al.

Over ten years ago, C. A. Mead and co-workers[3] demonstrated that on many semiconductors, the barrier heights of the common metals can be ranked, or ordered, by the Pauling electronegativity scale (see fig. 3 and 4). Figure 4 shows the Pauling electronegativity scale[3]

Figure 2. The range of barriers available on n- ZnS using just the elemental metals. The barrier heights of Al and Au represent the extremes of behavior of common elemental metal contacts. Of all the elemental metals, Au, the most electronegative, produces the highest barriers to n-type semiconductors.

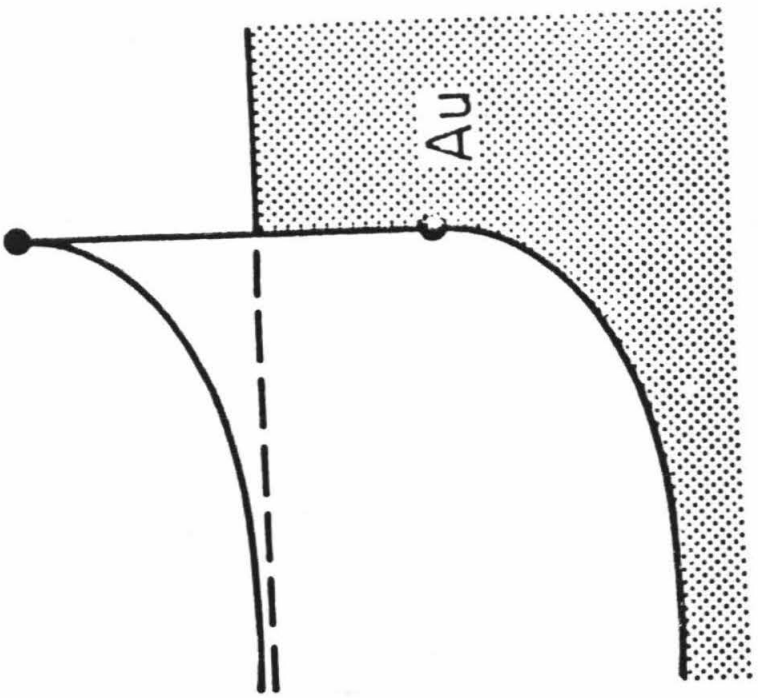
Au

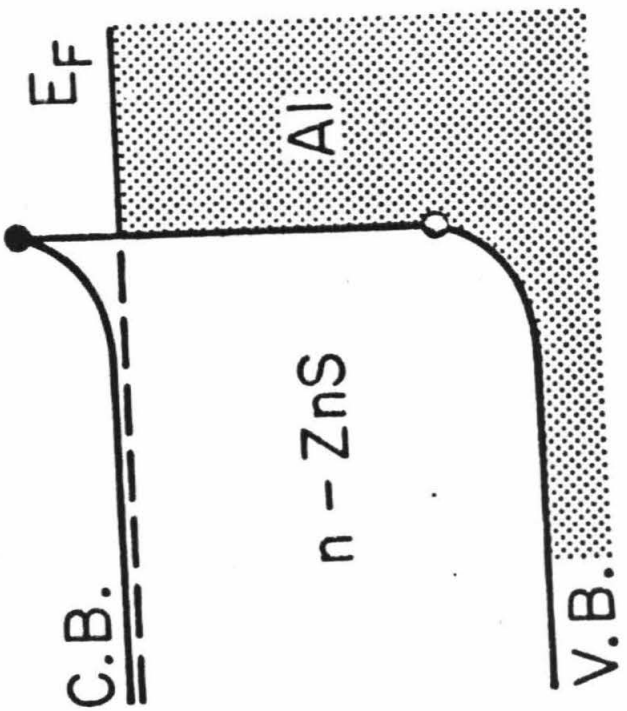
E_F
Al
n – ZnS
C.B.
V.B.

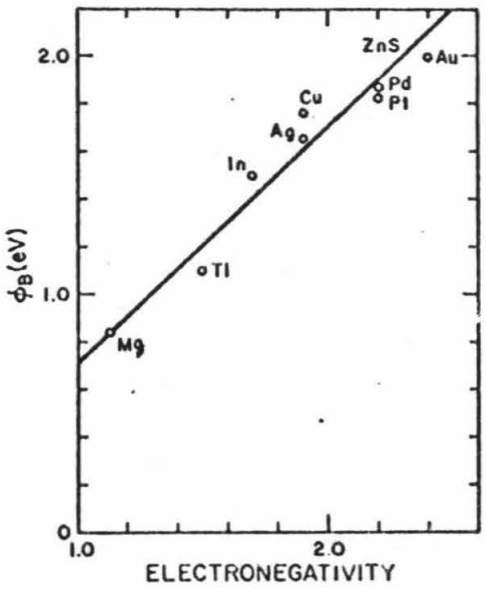

Figure 3. Barrier heights, ϕ, in eV vs. metal electronegativity, χ, for several elemental metals on n-type ZnS (after Reference 1).

Figure 4. The heights of barriers produced by the elemental metals can be ranked by the electronegativity of the metal. At the bottom are the Pauling electronegativity scale and some representative elements. The common metals occupy only a short range of the electronegativity scale. However, there exist metallic compounds which extend the available range of barrier heights. The very electronegative metallic compounds produce higher barriers to n-type semiconductors and lower barriers to p-type semiconductors than do the elemental metals.

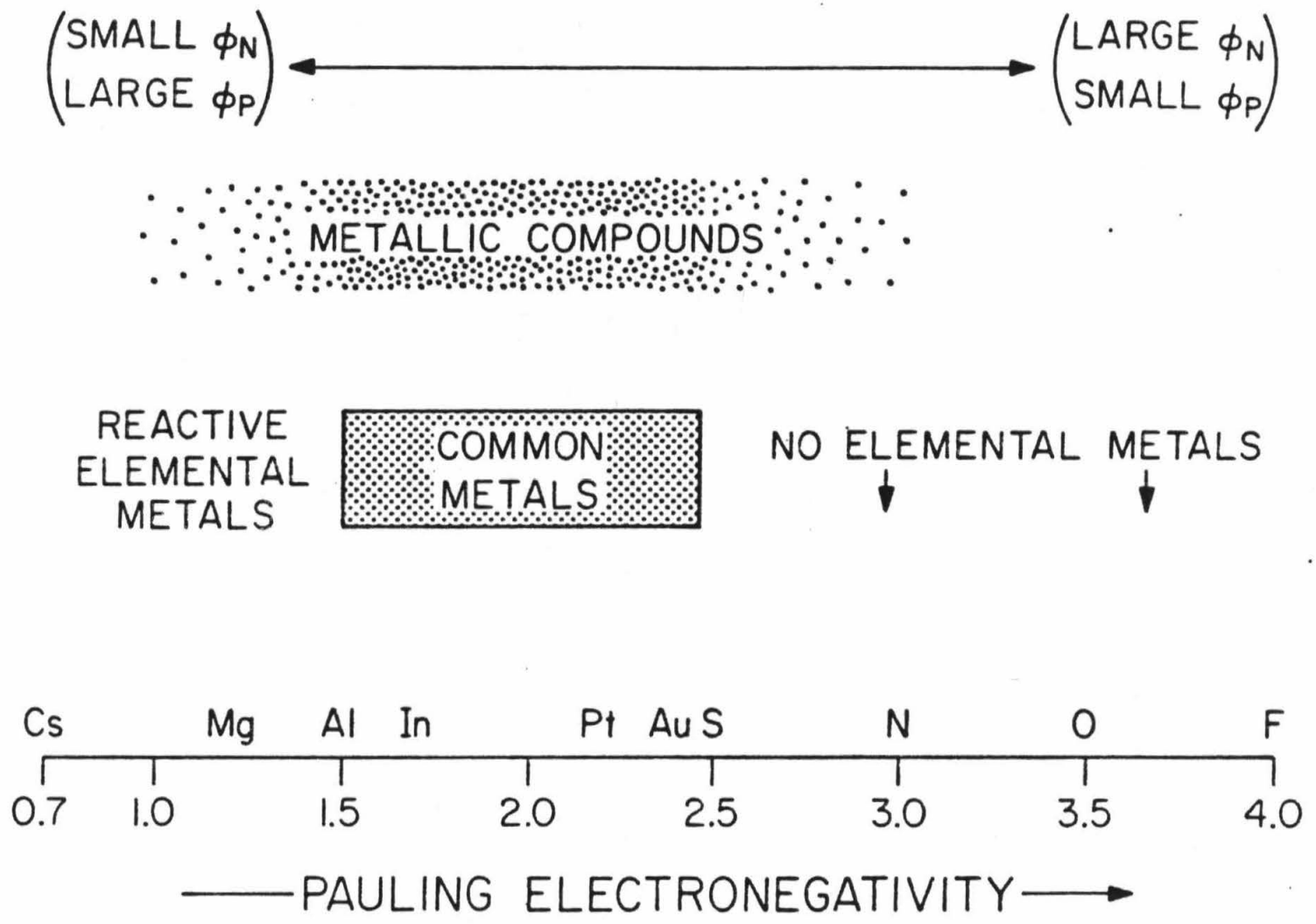
(SMALL ϕ_N LARGE ϕ_P)
(LARGE ϕ_N SMALL ϕ_P)
METALLIC COMPOUNDS
REACTIVE ELEMENTAL METALS
COMMON METALS
NO ELEMENTAL METALS
Cs
Mg
Al
In
Pt
Au
S
N
O
F
0.7
1.0
1.5
2.0
2.5
3.0
3.5
4.0
PAULING ELECTRONEGATIVITY

and a number of representative elements. To the right are the very electronegative elements. Electronegative conductors tend to produce high barriers to n-type semiconductors. The commonly used elemental metals occupy a short range on the electronegativity scale, from Al at 1.5 to Au at 2.4. Actually, there are a number of more electropositive metals which produce lower barriers to n-type semiconductors than the commonly used metals; unfortunately, these metals are very reactive. Of all the elemental metals, Au, the most electronegative metal, produces the highest barrier to n-type semiconductors.

A limitation to the usefulness of Schottky barriers is the limited range of barrier heights available with the elemental metals. In many cases, we would like to produce contacts that are even more electronegative than Au. Such contacts would tend to produce higher barriers to n-type semiconductors and tend to produce ohmics to p-type semiconductors. There are only eight elements more electronegative than Au; not one is a conductor. In order to find a more electronegative contact we have to consider compounds. Figure 4 schematically indicates that metallic compounds may extend the range of barrier heights.

There are many metallic compounds. Unfortunately, the theory of the energy band relationships at a metal-semiconductor interface is not sufficiently developed to help choose a candidate material. Instead, we rely upon

the phenomenological rules developed by Mead and co-workers.[1]

Sulfur and nitrogen are very electronegative insulators. However, a binary compound of these elements, polymeric sulfur nitride, $(SN)_x$, is a conductor. $(SN)_x$ is composed of long chains of alternating sulfur and nitrogen atoms. It is a gold brown, solid metallic conductor which can be grown as a crystal or deposited as a thin film.[4,5] $(SN)_x$ was chosen as a possible candidate for an electronegative contact material.

This study sought to show that metallic compounds could extend the range of barrier heights beyond that of the elemental metals. A sufficient proof would be that $(SN)_x$ produces higher barriers to n-type semiconductor than Au. Knowing this, one would then expect $(SN)_x$ to also produce smaller barriers or perhaps ohmics to p-type semiconductors. I undertook a study of the barrier heights of $(SN)_x$ and Au on ten different compound semiconductors.

B. Sample Preparation and Barrier Height Measurement

$(SN)_x$ was prepared in an apparatus similar to Mikulski et al.[4] by pumping S_4N_4 vapors past silver wool at 220°C and collecting the resultant S_2N_2 on a 77°K cold finger in a diffusion pump system. The cold finger was warmed to room temperature and polymerization of the

S_2N_2 to produce $(SN)_x$ was carried out for two days. Resultant $(SN)_x$ was heated to 85°C in vacuum to remove S_4N_4. Films were grown from (1) this powdered $(SN)_x$, (2) powder that had been washed in CH_3Cl to extract S_4N_4, and (3) crystals that were formed by heating the powdered $(SN)_x$ in vacuum and then condensing $(SN)_x$ on a cold finger.

$(SN)_x$ films were deposited[5] onto crystalline semiconductor substrates using a glass sublimator. Substrates were held against a cold finger using a clip. The $(SN)_x$ was 16 cm distant, at the bottom of a tube. During vacuum pump-down, the cold finger was heated to approximately 50°C. After one hour of vacuum pumping, the lower 5 cm of the $(SN)_x$ tube was placed into a 140°C oil bath and then the cold finger was water cooled to 10°C. Using powder $(SN)_x$ as a source, the time to deposit an opaque film on the glass cold finger containing the semiconductor substrate was approximately 20 minutes; using crystalline $(SN)_x$ as a source, the time increased to several hours. When powdered $(SN)_x$ was used as the source, a narrow orange-yellow ring, about one to three mm high, deposited on the inside of the sublimator tube several cm above the oil bath surface; this may have been S_4N_4. Material that had been washed in CH_3Cl to extract S_4N_4 produced a much more transparent ring; crystalline $(SN)_x$ did not produce a visible orange-yellow deposit. Significant amounts of $(SN)_x$ were deposited on the sublimator tube in the

region above the yellow ring; however, the glass tube in the region of the cold finger remained clean. The cold finger itself received a thin deposit of $(SN)_x$. $(SN)_x$ was deposited only if the cold finger was cooled below room temperature. Decreasing sample to source distance may decrease material loss at the risk of increased film contamination. The slight heating of the substrate during vacuum pump-down was found necessary to keep interfaces free of an insulating film. Very thick $(SN)_x$ films ($\sim$10 um) tended to have adhesion problems, either to the substrate or internally.

No difference in electrical characteristics was noted between films made with $(SN)_x$ purified in different ways. Most of the results reported here used CH_3Cl-washed powdered $(SN)_x$ for the following reasons: (1) the transport procedure used to make crystalline $(SN)_x$ involved significant material loss, (2) the deposition of films using crystalline $(SN)_x$ required that the growing film be exposed to the poor vacuum of an oil pumped system for several hours, (3) unwashed powdered $(SN)_x$ caused vacuum system pressure to increase significantly during initial immersion of the sublimator tube in 140°C oil.

Processing and measurement of the Schottky barriers on the various semiconductors proceeded generally as follows. Crystals were obtained in boule or (100) wafer form. Boules were oriented to a cleavage plane, sliced and sometimes annealed to proper carrier concen-

tration to produce material with high enough conductivity to permit meaningful I-V and C-V measurements, but still low enough to prevent tunneling. Ohmics were made on a cleaved surface or on a mechanically abraided surface that had been etched with a methanol-bromine solution. Fine wires were In soldered to the ohmics prior to the final cleave. Schottky barriers were formed with Au by (1) cleaving in vacuum in an evaporating stream of Au, (2) cleaving in air and immediately placing in the vacuum system, and occasionally, (3) cleaving in air and waiting an hour before placing in vacuum system. Evaporations were carried out at about 2.7×10^{-5} Nm^{-2} (2×10^{-7} Torr) in an oil-free system. No difference in barrier height for Au was noted between the two types of air-cleave. Vacuum cleave was done to test experimental technique and measurements against previously published results for Au barriers.[1] Agreement was good. Sample to sample reproducibility of Au barrier height determinations was about 0.05 eV.

An $(SN)_x$ sample and a control Au sample were made simultaneously. The semiconductor was cut into the shape of a bar, with a cleavage plane perpendicular to the length of the bar. Two ohmics were made, and tested for linearity. The sample was cleaved in air; one resulting piece was placed in the $(SN)_x$ film sublimator, the other set aside. After $(SN)_x$ film deposition, the two samples were

placed side by side in an ion-pumped system and several hundred Å of Au were evaporated onto the samples through a metal screen. The Au film on top of the $(SN)_x$ film served two purposes: to provide a low resistance contact to the $(SN)_x$ film and to protect the $(SN)_x$ film from water vapor in the atmosphere. Individual $(SN)_x$ diodes were then isolated by scribing the $(SN)_x$ film under a microscope. $(SN)_x$ barrier measurements on diodes isolated by using the Au as a mask and etching the $(SN)_x$ in dilute HNO_3 did not appear to be as reproducible as scribed diodes.

Barrier heights were measured[1] by photoresponse, current voltage (I-V), and capacitance-voltage[6] (C-V) techniques. A summary of barrier height measurements and details of the respective sample preparation are presented in Table I.

Experience with elemental metal barriers on various semiconductors has shown the photoresponse technique to be the most reliable and reproducible method of barrier height determination. The interface is illuminated with chopped monochromatic light and the short circuit photocurrent is measured by a phase-sensitive amplifier. Photons of energy $h\nu$ are absorbed in the conductor and produce excited carriers of energy ranging from about $E_F - kT$ to about $E_F + h\nu + kT$, where k is the Boltzmann constant, T is Kelvin temperature, and E_F is the Fermi

Table I. Comparison of Au and $(SN)_x$ Schottky Barrier Heights in eV on Semiconductors Cleaved in Air.

Semiconductor	n-GaAs	p-GaAs	n-InP	p-GaP	p-ZnTe	n-CdSe	n-ZnSe	n-CdS	n-ZnS
$N(cm^{-3})$	1.3×10^{17}	1.2×10^{17}	1×10^{17}	1.8×10^{17}	2.1×10^{16}	1×10^{15}	5×10^{17}	4.5×10^{17}	5×10^{16}
Anneal	none	none	none	none	700°C Te vapor	750°C Se vapor	750°C liq. Zn	none	880°C liq. Zn
Ohmics	Ge-Ni-Au	Au-Zn	In	Au-Zn	Li, Au	In	Hg-Cd-In	In	Hg-Cd-In
ϕ(Au) photo	.9	.4	.4 to .5	.7	.6 to .9	.6	1.35	.8	1.9
C-V	.9	.5	.5	.8	.8	NR	1.6	.8	1.9
I-V	.9	.4 to .5	.5	.7	.6	.5	1.3	.8	1.8
$\phi(SN)_x$ photo	1.2	ohmic	.8 to .9	NA	ohmic	.7	1.7	1.1	2.9 to 3.0
C-V	NR	.4	.8	.6	NR	NR	NR	1.1	3.0
I-V	1.0	.3 to .4	.8	NR	.3 to .4	.6 to .7	1.9	NR	2.7
$\phi(SN)_x - \phi$(Au)	.1	-.1	.3	-.2	-.3	.1 to .2	.3 to .6	.3	.9 to 1.0

N: Net carrier concentration
NR: Not reliable
NA: Not attempted

energy. Consider a barrier of barrier height ϕ. Carriers of energy less than $E_F + \phi$ soon relax back to the Fermi level and produce no net photocurrent. Some of the carriers with energy greater than $E_F + \phi$ diffuse across the interface and contribute to the photocurrent. Extrapolation of the square root[7] of the photocurrent gives ϕ (see Fig. 5).

For $h\nu > E_G$, a very large current is also produced by band to band excitation in the semiconductor. Thus scattered white light of very low intensity can obscure the conductor photoemission. By illuminating the metal through the semiconductor, almost all photons of energy greater than E_F are absorbed before reaching the interface. Thus by using a configuration in which the monochromater output is transmitted through the semiconductor, the Schottky barrier conductor to semiconductor excitation can be separated from the band to band excitation.

Most semiconductors showed another type of internal excitation for photon energies less than the band gap. This response almost obscured the conductor photoemission in some ZnS diodes. This excitation is probably related to the weak absorption below the band gap (Urbach's Rule) that is characteristic of many different insulators and semiconductors. Dow and Redfield[8] have presented an explanation for Urbach's Rule in terms of high microfields which enable tunneling from an exciton state to the band edge.

Figure 5. Photoresponse determination of barrier height. The square root of short circuit photocurrent per photon is plotted against photon energy for a typical Au/n-GaAs diode. The interface is illuminated through the GaAs. Region I shows the extrapolation to the barrier height, ϕ_n. Region II indicates a below band gap absorption in the semiconductor. Virtually all the photons in region III are absorbed in the bulk of the semiconductor and do not reach the Au/n-GaAs interface.

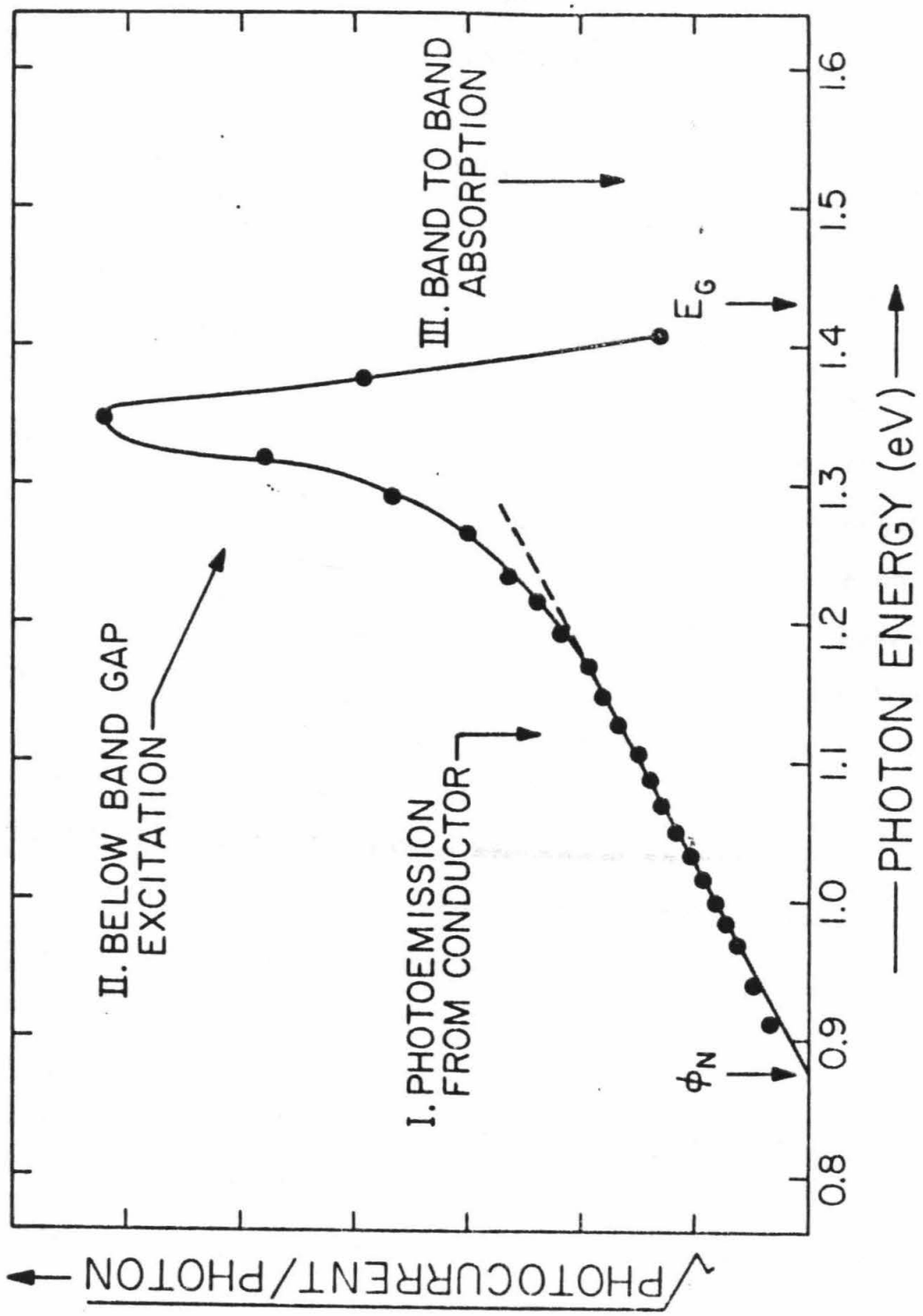
PHOTOCURRENT/PHOTON
PHOTON ENERGY (eV)
0.8
0.9
1.0
1.1
1.2
1.3
1.4
1.5
1.6
I. PHOTOEMISSION FROM CONDUCTOR
II. BELOW BAND GAP EXCITATION
III. BAND TO BAND ABSORPTION
ϕ_N
E_G

The measurement of the barrier height by the photoresponse technique was made using a quartz prism monochromater. The light source was a tungsten filament lamp that was focused by a mirror, through a chopper, onto the input slits of the monochromater. The monochromatic light output of the unit was focused onto the Schottky diode using an elliptical mirror. Sample movement into the focused light spot, as well as movement of the sample probe, was made with micrometer screws. Verification of the manufacturer's specified dispersion and wavelength calibration was made with a 6328 Å He-Ne laser and a Hg line source. Calibration of the energy output vs. wavelength was made with a thermopile. The signal current was synchronously detected and measured with a system having a full scale sensitivity of $1\mu V$ maximum. Representative photoresponse plots are shown in Fig. 6.

The I-V technique of determining barrier height makes use of the exponential dependence of current density, J, on the applied voltage, V:

$$J = J_0 \exp\left[-q\phi/kT\right]\left[\exp\left(qV/nkT\right)-1\right]$$

Thus by plotting the logarithm of the current density against applied voltage, the barrier height could be determined[1]. The value for the barrier height determined by this technique was the same for data taken at 77°K as for data taken at 300°K and was in substantial agreement with the value for the barrier height as deter-

Figure 6. Photoresponse determination of barrier energies. The square root of short-circuit photoresponse (arbitrary units) is shown as a function of photon energy for Au and $(SN)_x$ barriers on (a) n-ZnS, and (b) n-ZnSe. Dashed lines show the extrapolation used to obtain the barrier energy of each structure. $(SN)_x$ has a barrier of 2.9 eV on ZnS and 1.7 eV on ZnSe.

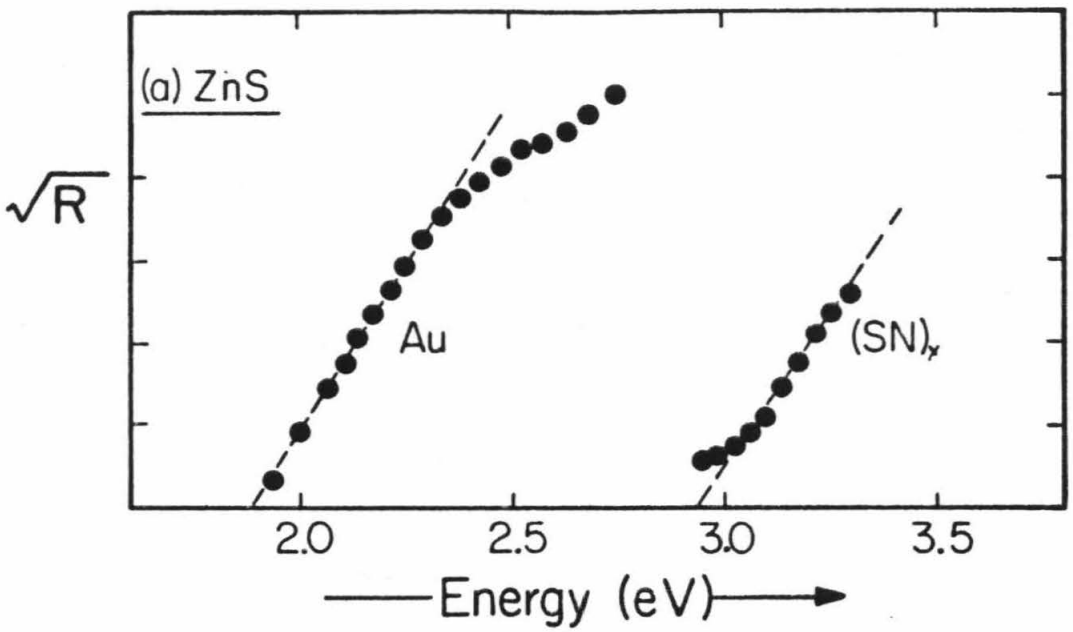
(a) ZnS
√R
Au
(SN)x
2.0
2.5
3.0
3.5
Energy (eV)

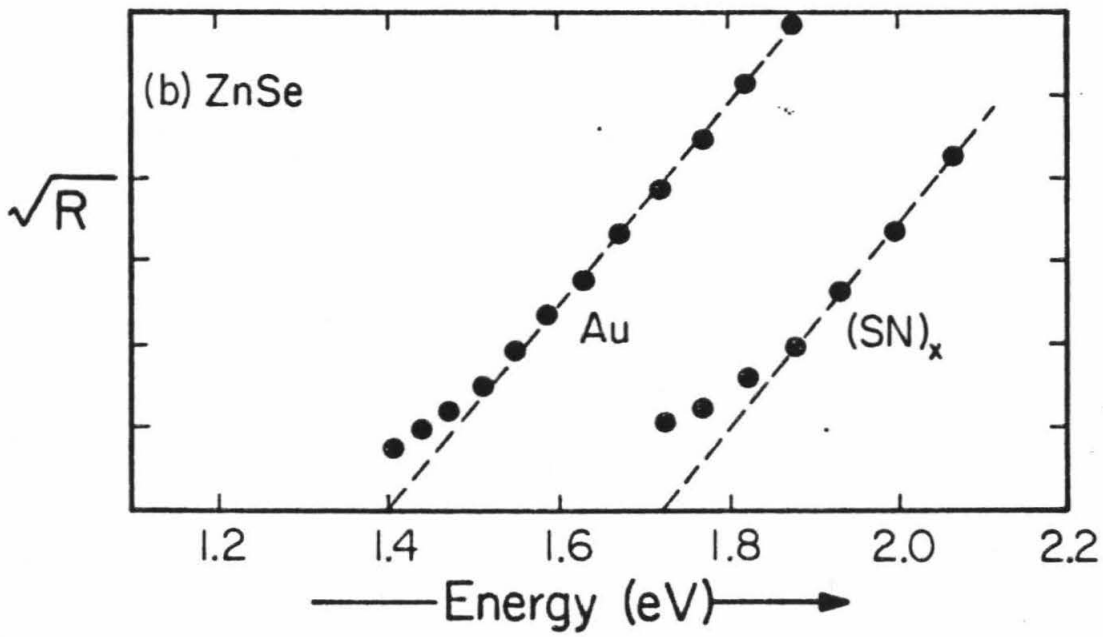
(b) ZnSe
√R
Au
(SN)x
1.2
1.4
1.6
1.8
2.0
2.2
Energy (eV)

mined by C-V and photoresponse techniques.

All I-V data were taken in the dark, with the exception of n-CdSe measurements and a set of photovoltage measurements on n-GaAs. The n-CdSe diodes showed high series resistance due to low carrier concentration. In order to decrease series resistance, I-V measurements on CdSe were made under white light. As the resulting photo-cell had an open circuit voltage of less than 2×10^{-4} V and a short circuit current of less than 10^{-6} A/cm^2, the I-V technique was still a valid method of determining barrier height. For several of the n-GaAs diodes, the increase in barrier height, $\phi(SN)_x - \phi(Au)$, was also measured by the increase in open circuit photovoltage when exposed to intense white light. The $(SN)_x$/n-GaAs diodes produced an open circuit saturation photovoltage of 0.12 V higher than Au/n-GaAs diodes.

A third technique to determine the barrier height is to measure the capacitance as a function of bias.[6] This information also gives the carrier concentration of the semiconductor. A problem with this technique, however, is the existence of trapping centers deep within the gap of the semiconductor. The charging and discharging of these traps affects the measured capacitance. The deep traps can have long time constants and can be charged and discharged by incident light as well as by the applied voltage. To minimize these effects, capacitance-voltage measurements

were taken in the dark, returning to zero bias between measurements. However, the capacitance of some diodes drifted with time and showed a dependence on the history of voltage bias of the diodes. Fortunately, the C-V measurements at 77°K typically showed less influence of traps. Representative C-V plots are shown in Figure 7.

No one method of barrier height determination was considered conclusive. Interfacial layers and tunneling can interfere with I-V barrier determination; traps, interfacial layers, and high series or low shunt resistances can interfere with C-V barrier determination; scattered light and near band gap excitations can interfere with photoresponse determination. However, the combination of techniques, especially at different temperatures, can be quite informative. When a barrier height measurement suffered from one of the above problems, or did not prove to be reproducible, the corresponding entry in Table I is listed as "not reliable".

Assignment of a barrier height for CdTe proved difficult, possibly as a result of the high chemical reactivity of the surface (see Table II). Gold barriers to vacuum cleaved n-CdTe measured .56 eV (photoresponse) and .6 to .65 eV (C-V), in approximate agreement with published .60 and .71 eV values.[1] Cleaving in air increased the barrier height by 0.2 to 0.3 eV, a substantial change compared to other semiconductors. This variation suggests that the surface reacts with air. In

Figure 7. Capacitance-voltage determination of barrier energies of $(SN)_x$ and Au barriers on n-ZnS. Intercept on voltage axis plus a small correction gives barrier energy.

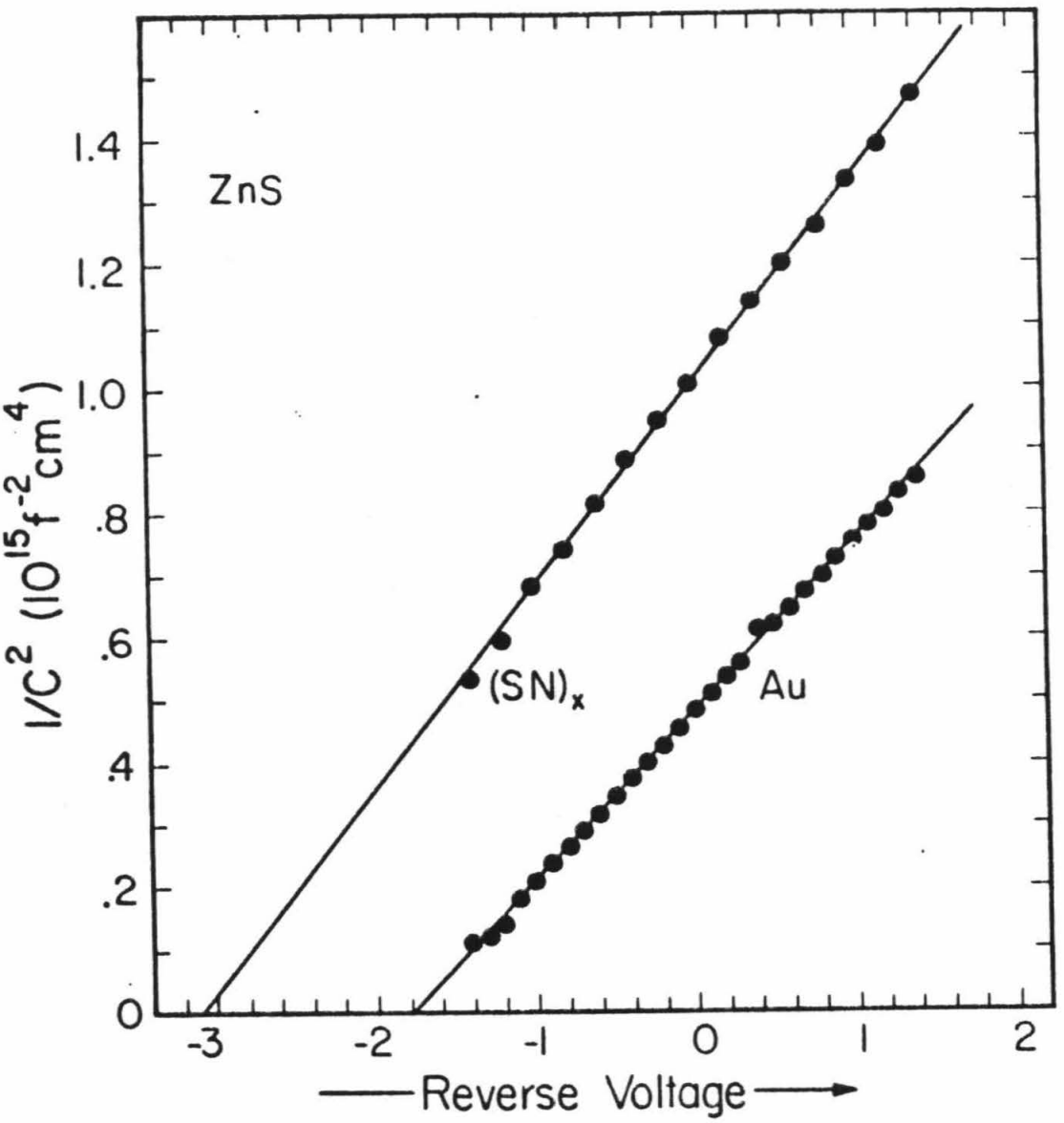
ZnS
(SN)x
Au
1/C² (10¹⁵f⁻²cm⁴)
1.4
1.2
1.0
.8
.6
.4
.2
0
-3
-2
-1
0
1
2
Reverse Voltage

Table II.

Measured barrier heights for Au on CdTe (eV)

	n-type	p-type
vacuum cleave	.5 to .6 (photo)	.5 to .6 (photo)
	.6 (C-V)	
air cleave	.6 to .8 (photo)	.6 (photo)
	.7 to .9 (C-V)	

agreement, secondary ion mass spectrometry measurements have shown a CdO layer at the interface of air-cleaved and chemically etched CdTe barriers.[9] In addition, Au barriers on CdTe do not appear to follow the relation $E_G = \phi_n + \phi_p$, where ϕ_n is the barrier to n-CdTe and ϕ_p is the barrier to p-CdTe, probably as a result of the formation of gold tellurides at the interface. Gold tellurides have been observed on CdTe regardless of the Au deposition method.[9,10] An energy band diagram has been suggested for the resulting Au_xTe/CdTe heterostructure.[11]

C. Discussion

Barrier heights for Au contacts to air cleaved semiconductors were compared to barrier heights for $(SN)_x$ contacts. By three methods of barrier height measurement, $(SN)_x$ was shown to produce more electronegative contacts than Au. Table I shows the difference between the barrier heights for $(SN)_x$ and for Au. Of all the elemental metals, Au produces the highest barriers to n-type semiconductors. $(SN)_x$ produces higher barriers than Au and therefore higher barriers to n-type semiconductors than any elemental metal. Of all the elemental metals, Au produces the lowest barriers to p-type semiconductors. For p-type semiconductors, $(SN)_x$ produces lower barriers than Au. Sometimes the resulting ohmic contact prevented determin-

ation of the barrier height at room temperature.[1] Thus $(SN)_x$ extends the available range of barrier heights. $(SN)_x$ positions the Fermi level at the interface closer to the valence band maximum than any elemental metal (see fig. 8).

As mentioned before, several phenomenological rules have been noted for the variation of Schottky barrier height of elemental metals on compound semiconductors. Indeed, the increase in ϕ_n with increasing electronegativity of the metal was used to choose $(SN)_x$ as a candidate for a contact to produce a large ϕ_n. The $(SN)_x$ data can also be examined in terms of two other major trends: the ionic-covalent transition, and the correlation of barrier height with the anion of the semiconductor. The ionic-covalent transition[12] pertains to the abrupt change in certain electronic properties of a large number of materials as ionicity increases. In Fig. 9, the variation in barrier height with metal electronegativity, $S = d\phi/d\chi_m$, is plotted against semiconductor ionicity, defined as $\Delta\chi = \chi(\text{anion}) - \chi(\text{cation})$ using the Kurtin, McGill and Mead[12] data. A similar plot of the barrier height difference between Au and $(SN)_x$, $|\phi(SN)_x - \phi(Au)|$ versus $\Delta\chi$ is also shown in Fig. 9. Clearly, barriers formed with $(SN)_x$ follow the ionic-covalent transition.

An estimate of the effective electronegativity of $(SN)_x$ for use in predicting barrier height on other mater-

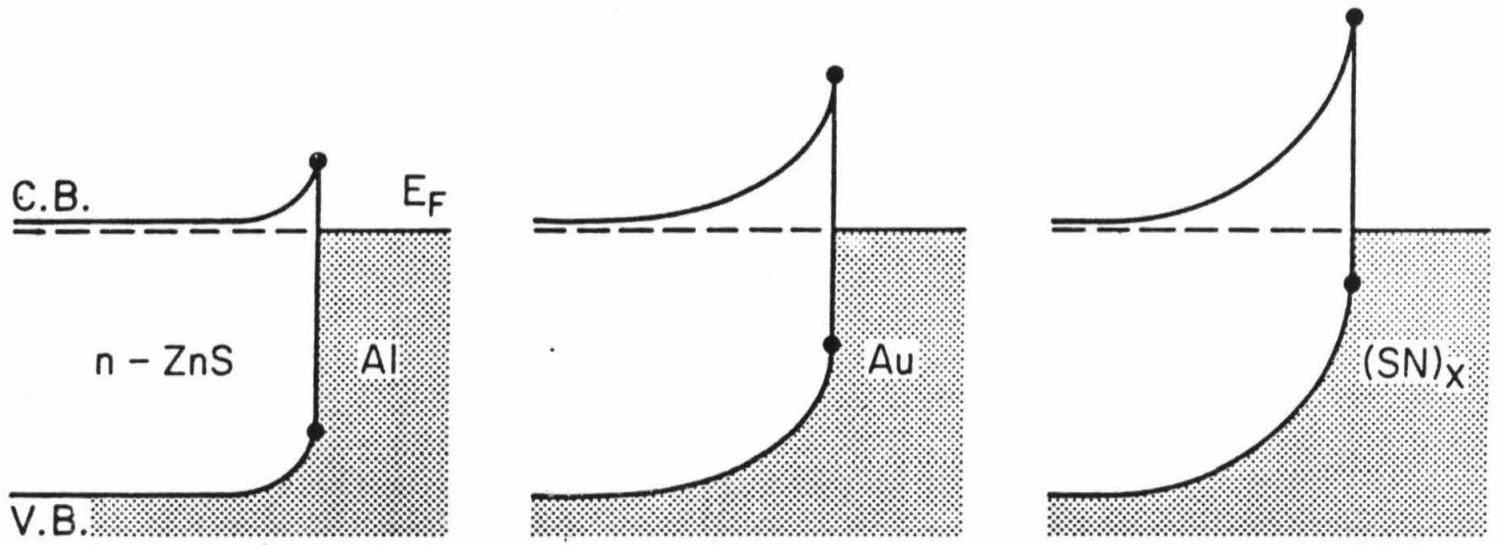

Figure 8. A comparison of the barrier heights of polymeric sulfur nitride and of the elemental metals Au and Al on n-ZnS.

Figure 9. The ionic-covalent transition. (a) The variation, δ, in barrier height with metal electronegativity for common compound semiconductors is plotted as a function of semiconductor ionicity, (from ref. 12). (b) The difference between barrier height for $(SN)_x$ and barrier height for Au, also plotted against semiconductor ionicity.

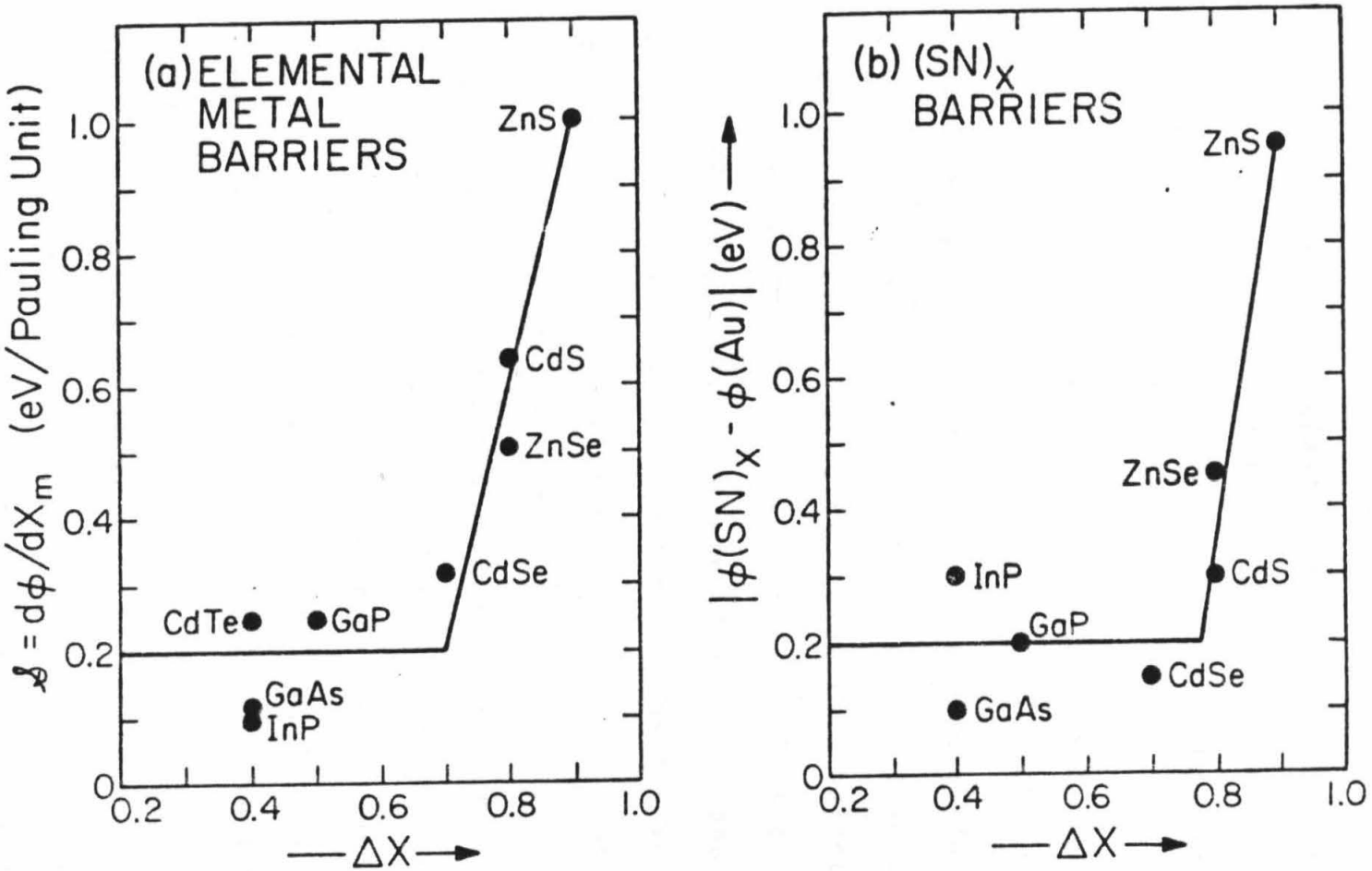
(a) ELEMENTAL METAL BARRIERS
$S = d\phi/dX_m$ (eV/Pauling Unit)
ZnS
CdS
ZnSe
CdSe
CdTe
GaP
GaAs
InP
0
0.2
0.4
0.6
0.8
1.0
0.2
0.4
0.6
0.8
1.0
—ΔX→
(b) $(SN)_X$ BARRIERS
$|\phi(SN)_X - \phi(Au)|$ (eV) →
ZnS
ZnSe
CdS
InP
GaP
CdSe
GaAs
0
0.2
0.4
0.6
0.8
1.0
0.2
0.4
0.6
0.8
1.0
—ΔX→

ials could be obtained from a comparison of the δ parameter and the $\phi(SN)_x$ - $\phi(Au)$ data. A least square fit produces $\chi \sim 3$; however, this value should be used with caution, as there is much uncertainty in the determination.

An alternate ordering parameter is the conductor work function. For example, the simple Schottky[13] model of the energy band relationship at a metal/semiconductor interface uses the metal work function, rather than the metal electronegativity to predict the barrier heights. The work function approximately scales with electronegativity; the metals with high work function produce high barriers to n-type semiconductors. Thus the work function of $(SN)_x$ could be significantly higher than the work function of any elemental metal.

An important concept often linked to the ionic-covalent transition is that of surface states, proposed by Bardeen.[14] Surface states refer to an increase in the density of states within the energy gap, that arise from termination of the lattice. Subsequent investigation of Schottky barriers on a large number of semiconductors by Mead[1] suggested that there were two classes of semiconductors: those with surface states and those without surface states (later identified as ionic and covalent.)

To understand the effect of surface states on Schottky

barriers, perform the "gedanken" experiment of placing a metal plate in close proximity to a clean semiconductor surface. Following the Schottky model, there will be an electric field produced that is proportional to $W_m - W_s$, where W_m is the work function of the metal and W_s is the work function of the semiconductor. This electric field must terminate on charge. In the original Schottky model (no surface states), the charge resides at impurity atoms or defects in the semiconductor space charge region, resulting in a change in the semiconductor Fermi level. Metals of different workfunction would give different barrier heights. In the case of semiconductors with surface states, the induced charge resides in the surface states, resulting in little or no change in the Fermi level of the semiconductor. Thus semiconductors with surface states should show little variation in barrier height with metal workfunction or electronegativity, in agreement with the results on covalent semiconductors.

The modifications[15, 16] to this model have involved interface states rather than surface states. Interface states arise from the presence of the metal at the terminated lattice, i.e., they are not the same states as in the semiconductor/vacuum interface. In agreement with this concept, some experiment photo-emission work shows no states in the energy gap of a very clean GaSb surface. However, the addition of a metal

overlayer or 1% of a monolayer of O_2 produces states within the energy gap.[18]

The barrier height improvement afforded by $(SN)_x$ is placed in perspective in Fig. 10. At the left is a reproduction of a Au barrier height compilation by J. O. McCaldin, T. C. McGill and C. A. Mead.[19, 20] Briefly, it is a plot of the conduction band minimum and valence band maximum of the common III-V and II-VI semiconductors, using the Fermi level of Au, in a Schottky barrier structure, as a reference level. For example, the barrier height for Au on n-ZnS is 2.0 eV and the barrier height for Au on p-type phosphides and tellurides is about 0.8 eV. The data points represent a variety of investigators, surface preparation techniques, and measurement techniques. The important observation is that the barrier height for holes, ϕ_p, depends only on the anion of the semiconductor (the "common anion rule"). On the extreme right is an electronegativity scale of the elements.

This diagram can be used to estimate the barrier heights of other metals on these semiconductors. For example, the Fermi level of Al, at an interface with ZnS, would lie at approximately the position indicated by the electronegativity scale. The Fermi level of Al, at an interface with one of the more covalent semiconductors (to the left side of the diagram), would lie appreciably

Figure 10. At the left, the positions of the valence band maximums (hatched rectangles) and the conduction band minimums (shaded rectangles) of each semiconductor at an interface with Au are plotted using the Fermi level of Au as a reference level (after J. O. McCaldin, T. C. McGill and C. A. Mead, references 19, 20). To the right is an electronegativity scale of the elements. As described in the text, this diagram can be used to estimate the barrier heights of elemental metals on common compound semiconductors. The Fermi level of $(SN)_x$ lies below the Au reference level.

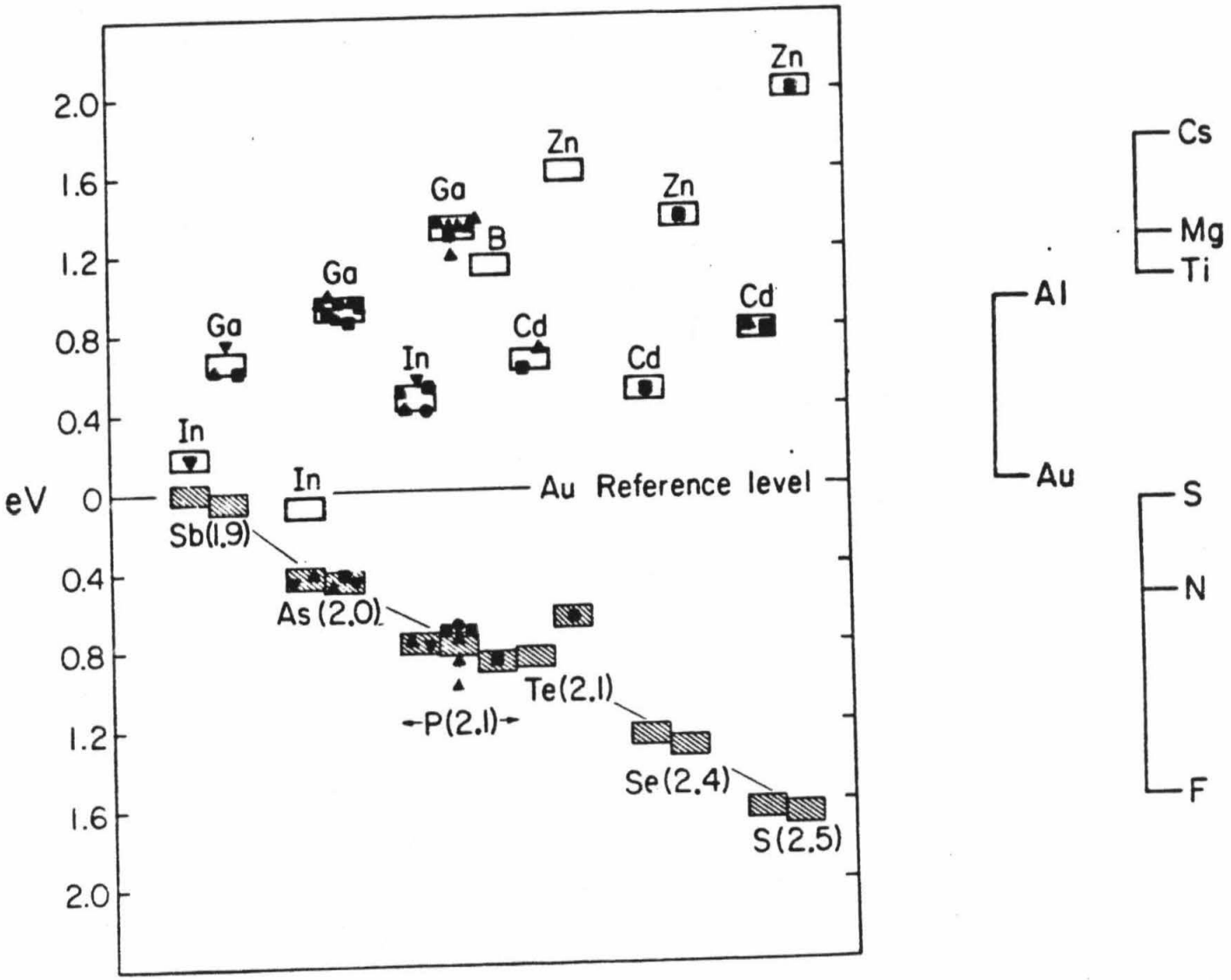
2.0
1.6
1.2
0.8
0.4
eV 0
0.4
0.8
1.2
1.6
2.0
Zn
Zn
Zn
Ga
B
Ga
Ga
Cd
Cd
Cd
In
In
In
Au Reference level
Sb(1.9)
As (2.0)
Te(2.1)
P(2.1)
Se(2.4)
S(2.5)
Cs
Mg
Ti
Al
Au
S
N
F

closer to the Au reference level, however. The Fermi levels of the other commonly used elemental metals would lie between the Fermi levels of Al and Au.

Notice that the Fermi level of the elemental metals, at the interface with many of these III-V and II-VI semiconductors, lies in the upper portion of the energy gaps. However, the lower portion of the energy gaps, below the Au reference level, cannot be contacted by the elemental metals. On this diagram, the Fermi level of $(SN)_x$ lies below that of Au, providing contact closer to the valence band maxima of these semiconductors.

Very electronegative conductors can be used to facilitate ohmic contacts to p-type semiconductors. An important way to make ohmics is to choose a conductor which produces a very low barrier height. Ohmics to n-CdS, n-CdSe, n-CdTe, and n-InP can be made with an electropositive elemental metal such as Al or In. The resulting small barrier produces an ohmic contact. On the other hand, the valence band maxima of the phosphides and tellurides lie well below the Au reference level. All the elemental metals produce relatively high barriers to the p-type phosphides and the tellurides. A very electronegative metallic compound would produce lower barriers to p-type semiconductors, thereby facilitating ohmic contacts to these semiconductors.

The common anion rule refers only to barriers formed by Au. However, the valence band maxima and conduction band minima of the various II-VI and III-V semiconductors

could also be plotted using the Fermi level of $(SN)_x$, in a Schottky barrier structure, as the reference level. This has been done (see fig. 11). Polymeric sulfur nitride does not follow the common anion rules; in this regard, Au is special.

Polymeric sulfur nitride is not likely to be of practical device use, because of instability in the presence of water vapor. Encapsulation may help. However, on the basis of early $(SN)_x$ work, and the anion systematics[19] of Schottky barrier heights, the author and coworkers predicted the existence of a number of very electronegative substances. One of these, a mercury chalcogenide, HgSe, has also been shown to be more electronegative than Au.[21] The mercury chalcogenides are likely to be useful in practice because of improved stability, compatibility with present semiconductor device processing, and ease of lattice match to II-VI and III-V compounds. Trends of the heights of Schottky barriers formed by $(SN)_x$ and the common tetrahedral III-V and II-VI compounds can be expected to carry over to other electronegative conductors. Thus HgSe will follow the ionic-covalent transition.[22]

D. Conclusions

The Schottky barrier heights of $(SN)_x$ on nine III-V and II-VI semiconductors have been determined. Polymeric

Figure 11. The maximum of the valence band of common II-VI and III-V semiconductors in contact with Au is plotted using the Fermi level of Au as a reference level. Also shown is the position of the $(SN)_x$ Fermi level relative to the valence band maxima. $(SN)_x$ does not follow the common anion rule. (Data for Au from reference 20).

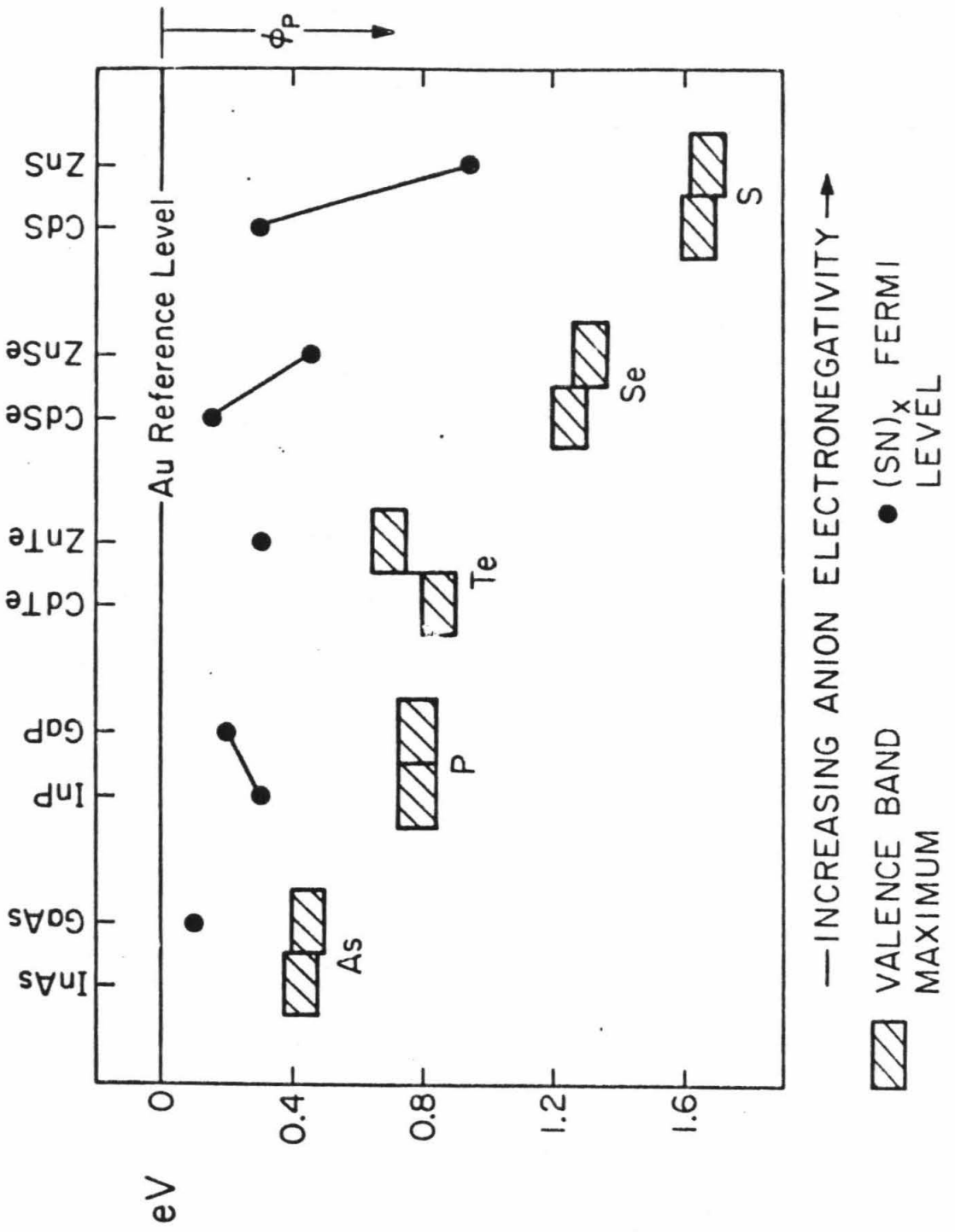
ϕ_P
Au Reference Level
InAs
GaAs
InP
GaP
CdTe
ZnTe
CdSe
ZnSe
CdS
ZnS
As
P
Te
Se
S
eV
0
0.4
0.8
1.2
1.6
INCREASING ANION ELECTRONEGATIVITY
VALENCE BAND MAXIMUM
$(SN)_x$ FERMI LEVEL

sulfur nitride produces higher barriers to n-type semiconductors and lower barriers to p-type semiconductors than any elemental metal. Thus, metallic compounds can be used to extend the range of barrier heights beyond those of the elemental metals.

Barriers produced with $(SN)_x$ follow the ionic-covalent transition; covalent semiconductors have a smaller barrier height change than ionic semiconductors. Contrary to the case of Au barriers, $(SN)_x$ barrier height does not depend solely on the anion of the semiconductor.

References

1. C. A. Mead, Solid-State Electron, 9, 1023 (1966)

2. S. M. Sze, Physics of Semiconductor Devices (Wiley, New York, 1969), pp. 410-412, 669

3. C. A. Mead, Phys. Lett. 18, 218 (1965)

4. C. M. Mikulski, P. J. Russo, M. S. Savan, A. G. MacDiarmid, A. F. Garito, and A. J. Heeger, J. Am. Chem. Soc. 97, 6358 (1975)

5. A. A. Bright, Marshal J. Cohen, A. F. Garito, A. J. Heeger, C. M. Mikulski and A. G. MacDiarmid, Appl. Phys. Lett. 26, 612, (1975)

6. Alvin M. Goodman, J. Appl. Phys. 34, 329 (1963)

7. R. H. Fowler, Phys. Rev. 33, 45, (1931)

8. John D. Dow and David Redfield, Phys. Rev. 135, 594 (1972)

9. P. Siffert, J. Berger, C. Scharager, A. Cornet, R. Stuck, R. O. Bell, H. B. Serreze, F. V. Wald, IEEE Trans. Nucl. Sci. N523, 163 (1972)

10. T. J. Magee, unpublished data

11. Y. Touskova and R. Kuzel, Phys. Stat. Sol. (a)15, 257 (1973)

12. S. Kurtin, T. C. McGill and C. A. Mead, Phys. Rev. Lett. 22, 1433 (1969)

13. W. Schottky, Z. Physik 118, 539 (1942)

14. J. Bardeen, Phys. Rev. 71, 717 (1949)

15. Volker Heine, Phys. Rev. A 138, 1689 (1965)

16. E. Louis, F. Yndurain and F. Flores, Phys. Rev B 13, 4408 (1976)

17. S. G. Louie, J. R. Chelikowsky and M. L. Cohen, J. Vac. Sci. Technol. 13, 790 (1976)

18. W. E. Spicer, I. Lindau, P. E. Gregory, C. M. Garner, P. Pianetta and P. W. Chye, J. Vac. Sci. Technol. 13, 780 (1976)

19. J. O. McCaldin, T. C. McGill, and C. A. Mead, Phys. Rev. Lett. 36, 56 (1976)

20. J. O. McCaldin, T. C. McGill, and C. A. Mead, J. Vac. Sci. Technol. 13, 802 (1976)

21. J. S. Best, J. O. McCaldin, T. C. McGill, C. A. Mead and J. B. Mooney, Appl. Phys. Lett. 29, 433 (1976)

22. R. A. Scranton, J. S. Best, and J. O. McCaldin, J. Vac. Sci. Technol. 14, 930 (1977)

II. The Dissolution Rate of Amorphous Silicon into Aluminum.

A. Introduction

Epitaxial growth is the process of producing thin film layers on a substrate so that the crystal structure of the film is an extension of the crystal structure of the substrate. In solid phase epitaxy (SPE), both the source and the growth medium are solid. The source is in the form of an amorphous layer. Growth is driven by the lower free energy of the crystalline film relative to the amorphous source.(1)

The SPE process is of potential interest to semiconductor device technology because of the low temperaatures often employed (300° to 600°C) compared to more conventional epitaxial growth processes (900°C to 1200°C). Low temperatures are attractive because the diffusivities of common dopants and impurities are reduced, resulting in more abrupt interfaces. In addition, the equilibrium concentration of defects is reduced at low temperatures.

An important SPE growth system that has attracted interest recently is a structure consisting of amorphous Si film on an Al layer on a crystalline Si substrate (a-Si/Al/x-Si). At temperatures below the Si-Al eutectic (577°C), the a-Si has been shown to dissolve into the Al film, transport through the Al, and grow epitaxially

at the substrate.

The transport of Si through thin films of Al has been studied by J. O. McCaldin and H. Sankur.[2] The transport has been shown to follow Ficks law, i.e., simple diffusion. The diffusivity of Si in thin film Al has been measured and shown to be enhanced by about one and one half orders of magnitude over the diffusivity in bulk Al. However, the diffusivity in solids is still some three to five orders of magnitude smaller than the diffusivity in liquids and gases used in more conventional epitaxial growth. Nonetheless, SPE growth can still be very fast because the characteristic transport distance in SPE (10^{-5} to 10^{-4} cm) is small compared to distances in more conventional epitaxial growth.

Indeed, the growth rate in SPE may be too fast. Fast growth rates can bury defects, such as metallic inclusions, in the epitaxial film. For example, R. L. Boatright and J. O. McCaldin[3] have shown that transport limited growth in SPE can cause pockets of Al to form in the epitaxial Si layer. These defects were found after heat treatment at 475° to 525°C for 10 to 20 minutes. G. Majni and G. Ottaviani[4] have demonstrated large area, uniform growth of Si using SPE by heat treating an a-Si/Al/x-Si structure for 10 hours at 450° 530°C. Such long times cause significant intermixing of the Si and Al films. Nevertheless, the epitaxial films

prepared by Majni and Ottaviani also contained Al inclusions.

One possible method to decrease the number of buried defects is to limit the supply rate of nutrient Si to the growing epitaxial film. In this way, the growth rate would be reduced, so as to prevent defects from being buried. The transport would no longer be the limiting process, enabling the growth of uniform films.

Cline and Anthony[5] have studied the migration of liquid metals through crystalline semiconductors under a temperature gradient. They found the migration rate for liquid Al, Au, and Ga in Si to be well described by a transport limited model (only the Ga/GaAs system was found to be dissolution rate limited.) In contrast, the dissolution rate of a-Si into solid Al was not known. The purpose of this investigation was to measure the dissolution rate of a-Si into solid Al, compare it to the transport rate, and determine if a dissolution limited SPE could be obtained at low temperatures.

B. Measurement of Amorphous Silicon Dissolution Rate.

The dissolution rate of amorphous Si into Al was measured by electron microprobe analysis after heat treatment at various temperatures.

Samples were prepared as follows. Single crystal, polished sapphire substrates were cleaned in organics,

a standard Si etch, a standard hydrogen peroxide based cleaning solution, rinsed in deionized water and dried in an oxygen atmosphere for one hour at 1000°C. The substrates were loaded into an oil free vacuum system. After reaching a pressure of 2×10^{-7} Torr, separately shielded Al and Si sources were premelted. The substrates, on a heavy Cu block on a rotating shutter, were moved first into the flux of evaporating Si. The a-Si film thickness was monitored with a quartz crystal microbalance. Within seconds after finishing the Si evaporation, the samples were moved into the flux of evaporating Al. The Al film thickness was measured by a Nomarski interferometer after removal from the vacuum system. A typical structure was x-Al_2O_3 (300μ)/a-Si (450 Å)/Al (5.5μ).

The vacuum system used in this work is very similar to those used in many of the reported SPE experiments.[1-4,6] Electron beam evaporation of Si in an ion-pumped system at pressures of approximately 10^{-7} Torr is quite standard. John A. Roth and C. Lawrence Anderson[7] have noted several improvements in the SPE of the system a-Si/Pd/x-Si by using an ultra high vacuum of 10^{-9} to 10^{-10} Torr. The emphasis in this investigation was on more standard SPE conditions and hence a standard vacuum system was used.

Samples were quickly brought to heat treatment

temperature by dropping them individually onto a heavy Cu block in an Ar atmosphere. To insure good thermal contact to the back of the sapphire, the surface of the Cu block was polished and wetted with liquid In. The temperature was stabilized to within 1°C with a thermocouple and a proportional controller. The temperature was monitored with a digital thermometer with 0.2°C resolution, calibrated at the melting points of In, Sn, and Zn.

After heat treatment, a Cu vacuum chuck was used to quench the samples. Visual examination indicated that the In (melting point 156°C) that adhered to the back of the substrate solidified as soon as the substrate flew from the heated block to the vacuum chuck. This procedure was timed by stopwatch to an accuracy of $\pm$ 0.2s. Within 1s, the substrates were then placed into cold water to ensure complete cooling to room termperature.

After quench, the Al film and any Si in the Al film were removed by etching for 2h in an etch containing phosphoric acid. This etch did not attack a-Si, as evidenced by the fact that a 200 Å thick a-Si film was not etched in 10^3h.

Heated and unheated control samples were then examined in the optical microscope, scanning electron microscope, and the electron microprobe. Three different heat treat regimes were noted. For high temperatures,

e.g. 525°C (10s), the 450 Å a-Si films were completely dissolved. At medium temperatures, such as 375°C (10s), the a-Si film was covered by a layer of irregular Si precipitates of approximately 1 μ size (see fig. 1). At low temperatures, such as 275° to 325°C (2.5 to 10s), the films were characterized by a uniformly thinned a-Si field with occasional isolated Si precipitates (see fig. 2). The thickness of the uniform field in these specimens was measured by comparing the strength of the Si kα x-ray fluorescence in the electron microprobe with the strength of the signal from the unheated control. Uniformity of the field was verified by SEM and electron microprobe measurements. Typical results are indicated in Fig. 3 for the specimens in the low temperature regime.

C. Discussion

The dissolution rate of an amorphous Si film into solid Al far exceeds that of the simple transport model. For example, the thickness of the a-Si film that dissolves in the Al in a transport (diffusion limited) model is

$$Q = \frac{2}{\sqrt{\pi}} \sigma \sqrt{Dt} \qquad (1)$$

where Q is the thickness of a-Si removed, σ is the solubility of Si in Al, D is the diffusivity of Si in Al, and t is the time. Using values of σ and D

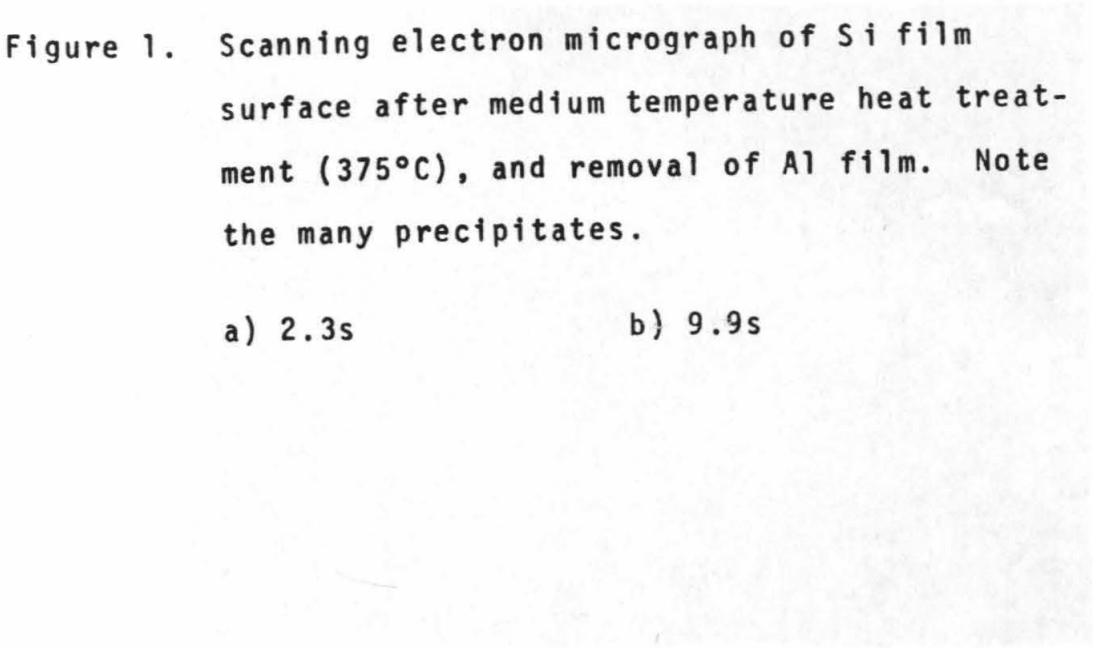

Figure 1. Scanning electron micrograph of Si film surface after medium temperature heat treatment (375°C), and removal of Al film. Note the many precipitates.

a) 2.3s b) 9.9s

1a)

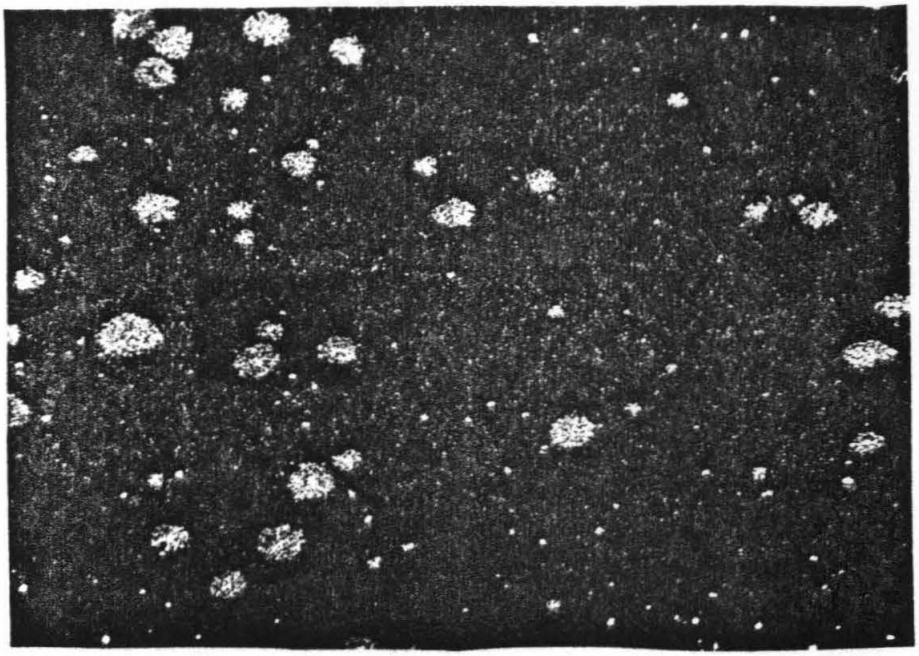

10 microns

1b)

Figure 2. Scanning electron micrograph of Si surface after low temperature heat treatment and removal of Al film. Note the isolated precipitates on a uniform field.

a) 2.5s b) 10s

2a)

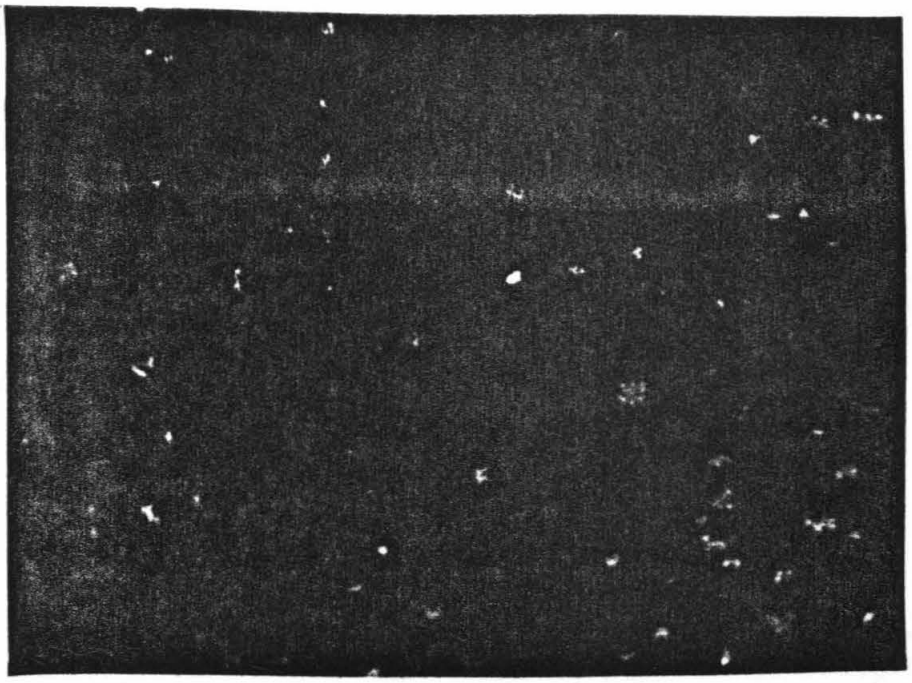

10 microns

2b)

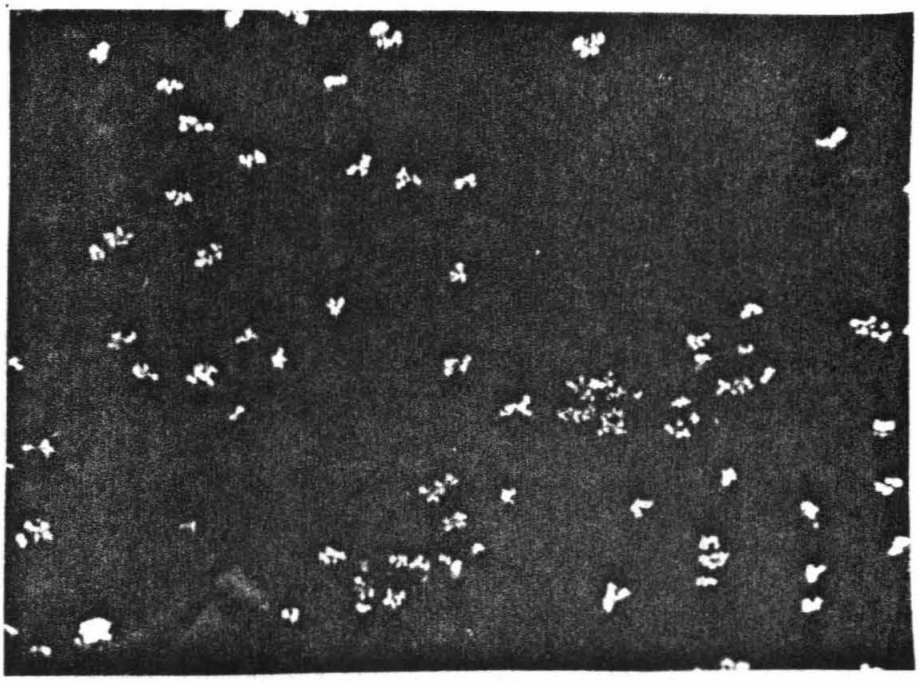

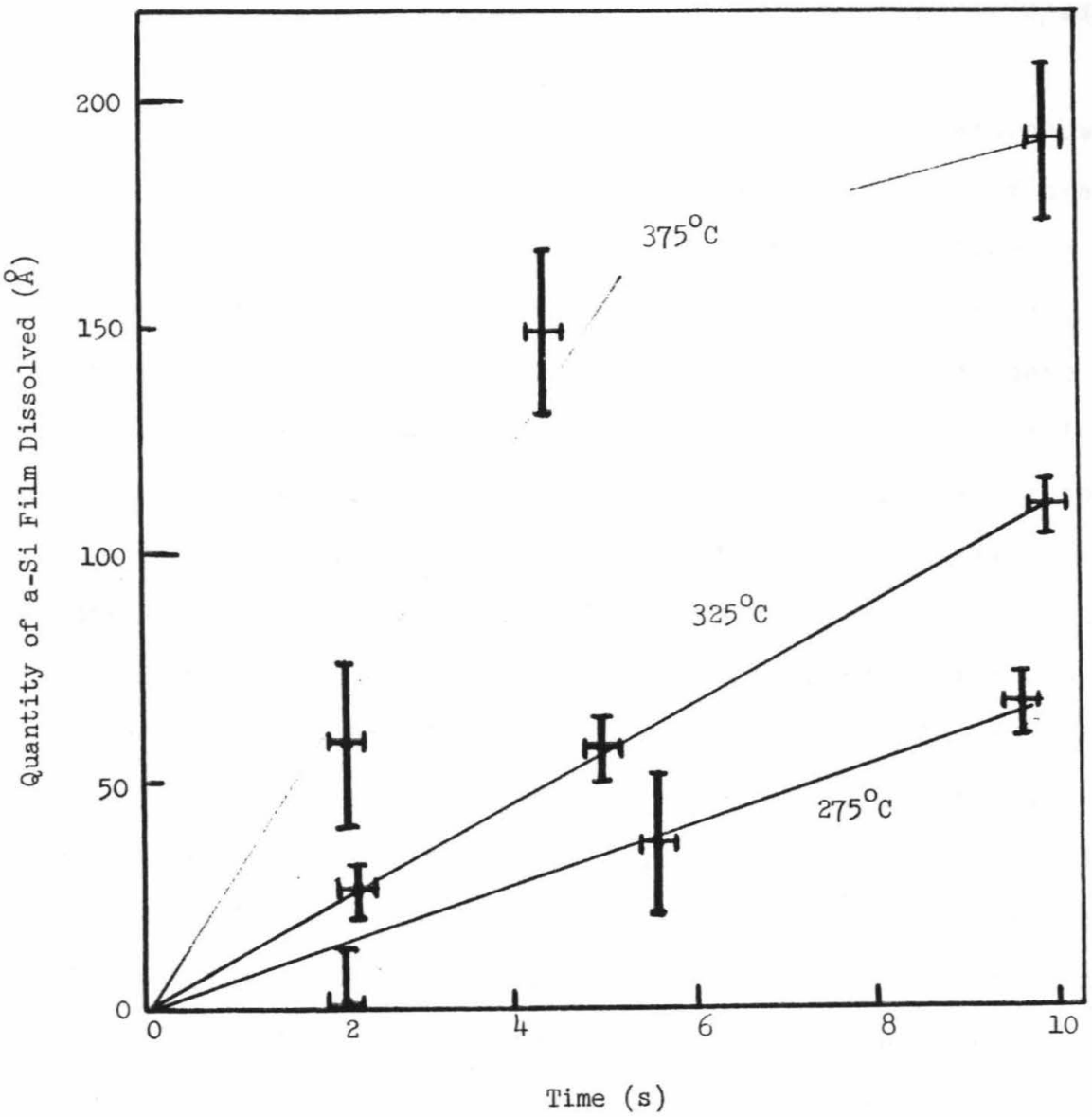

Figure 3. Thickness of amorphous silicon film removed by dissolution into a solid aluminum film as a function of time, with temperature of heat treatment as a parameter.

measured by McCaldin and Sankur, Q for the 325°C, 10s heat treat is 9 Å. In contrast, the electron microprobe indicates that 110 Å has actually been removed. The small quantity of precipitates at the surface does not account for the missing Si.

The present model is thus one of a nutrient amorphous Si film, with a high free energy, feeding a number of precipitates, with only a small quantity of Si dissolved in the Al. The precipitates are in the Al film as well as on the a-Si surface. The precipitates are a more ordered phase of Si than the amorphous film, and hence there is a net driving force for transport from the amorphous film to the precipitates.

The dissolution rate of a-Si into Al is initially constant and then decreases with time. The decrease of the dissolution rate correlates with the conversion of the a-Si field to Si precipitates. For example, the 375°C, 10s sample is almost totally covered with precipitates of the size 0.2 to 1.0μ. (see fig. 1). Correspondingly, the 375°C, 10s sample shows a lower etch rate than the 375°C samples heat treated for shorter times (see fig. 3). As the surface of the a-Si field changes to a more ordered phase, the driving force for dissolution of the Si into Al should decrease.

The present results confirm the transport limited growth observed by Boatright and McCaldin. In the case of longer heat treatment times (10h) used by Majni and

Ottaviani, the a-Si is likely to have been converted to a more ordered phase, with the later stages of transport occurring from low energy precipitates and growths to the very low energy crystalline film. However, as a result of the initial high dissolution rate of the a-Si in close proximity to the substrate, defects are likely to have been buried.

There are several possible remedies for the problem of the high initial dissolution rate burying defects during SPE growth. One would be to use polycrystalline Si, rather than a-Si, as the source material. The polycrystalline Si would have a lower driving energy to dissolve into the Al than would a-Si. A second remedy would be to use a barrier metal between the a-Si and the Al. This barrier would limit the supply of Si to the Al. Another idea is to use very thick Al films (10^{-3}cm instead of 5 X 10^{-5}cm thick films presently used). Thick Al would enable the a-Si to change into more ordered precipitates before diffusion has transported Si to the substrate.

D. Conclusions

The dissolution rate of a-Si into an evaporated Al film has been measured at low temperatures and shown to far exceed the transport rate. The results of SPE growth experiments are interpreted in terms of this result.

References--II

1. K. Nakamura, M. A. Nicolet, J. W. Mayer, R. J. Blattner, and C. A. Evans, Jr., J. Appl. Phys. 46, 4678 (1975)

2. J. O. McCaldin and H. Sankur, Appl. Phys. Lett., 19, 524 (1971)

3. R. L. Boatright and J. O. McCaldin, J. Appl. Phys. 47, 2260 (1976)

4. G. Majni and G. Ottaviani, Appl. Phys. Lett. 31, 126 (1977)

5. H. E. Cline and T. R. Anthony, J. Appl. Phys. 48, 2196 (1977)

6. J. M. Harris, R. J. Blattner, I. D. Ward, C. A. Evans, Jr., H. L. Fraser, M. A. Nicolet, and C. L. Ramiller, J. Appl. Phys. 48, 2897 (1977)

7. John A. Roth and C. Lawrence Anderson, to be published